AGU PUBLICATIONS

Geophysical Research Letters

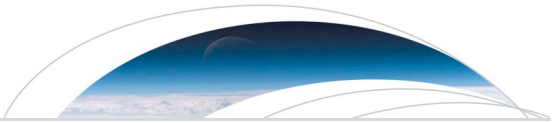

RESEARCH LETTER
10.1002/2017GL075711

Key Points:
- Electron scale magnetic peak is observed with the scale size of ~7 ρ_e (~0.06 ρ_i) in the magnetosheath
- Electron vortex is found perpendicular to the field line and the current system is consistent with the magnetic peak
- The magnetic peak is determined as magnetic bottle shape rather than flux rope by a new method

Supporting Information:
- Supporting Information S1

Correspondence to:
Q. Q. Shi and R. L. Guo,
sqq@pku.edu.cn;
grl@pku.edu.cn

Citation:
Yao, S. T., Shi, Q. Q., Guo, R. L., Yao, Z. H., Tian, A. M., Degeling, A. W., … Liu, H. (2018). Magnetospheric Multiscale observations of electron scale magnetic peak. *Geophysical Research Letters*, *45*, 527–537. https://doi.org/10.1002/2017GL075711

Received 20 SEP 2017
Accepted 22 DEC 2017
Accepted article online 29 DEC 2017
Published online 24 JAN 2018

Magnetospheric Multiscale Observations of Electron Scale Magnetic Peak

S. T. Yao[1,2], Q. Q. Shi[1], R. L. Guo[3], Z. H. Yao[4,5], A. M. Tian[1], A. W. Degeling[1], W. J. Sun[3], J. Liu[2], X. G. Wang[6], Q. G. Zong[7], H. Zhang[8], Z. Y. Pu[7], L. H. Wang[7], S. Y. Fu[7], C. J. Xiao[9], C. T. Russell[10], B. L. Giles[11], Y. Y. Feng[2], T. Xiao[1], S. C. Bai[1], X. C. Shen[1], L. L. Zhao[7], and H. Liu[7]

[1]Shandong Provincial Key Laboratory of Optical Astronomy and Solar-Terrestrial Environment, Institute of Space Sciences, Shandong University, Weihai, China, [2]State Key Laboratory of Space Weather, National Space Science Center, Chinese Academy of Sciences, Beijing, China, [3]Key Laboratory of Earth and Planetary Physics, Institute of Geology and Geophysics, Chinese Academy of Sciences, Beijing, China, [4]Mullard Space Science Laboratory, University College London, Dorking, UK, [5]Laboratoire de Physique Atmosphérique et Planétaire, STAR Institute, Université de Liège, Liège, Belgium, [6]Department of Physics, Harbin Institute of Technology, Harbin, China, [7]School of Earth and Space Sciences, Peking University, Beijing, China, [8]Physics Department and Geophysical Institute, University of Alaska Fairbanks, Fairbanks, AK, USA, [9]State Key Laboratory of Nuclear Physics and Technology, School of Physics, Peking University, Beijing, China, [10]Department of Earth, Planetary and Space Sciences, University of California, Los Angeles, CA, USA, [11]NASA Goddard Space Flight Center, Greenbelt, MA, USA

Abstract The sudden enhancements of magnetic strength, named magnetic peaks (MPs), are often observed in the magnetosheath of magnetized planets. They are usually identified as flux ropes (FRs) or magnetic mirror mode structures. Previous studies of MPs are mostly on the magnetohydrodynamics (MHD) scale. In this study, an electron scale MP is reported in the Earth magnetosheath. We present a typical case with a scale of ~7 electron gyroradii and a duration of ~0.18 s. A strong magnetic disturbance and associated electrical current are detected. Electron vortex is found perpendicular to the magnetic field line and is self-consist with the peak. We use multipoint spacecraft techniques to determine the propagation velocity of the MP structure and find that the magnetic peak does propagate relative to the plasma (ion) flow. This is very different from the magnetic mirror mode that does not propagate relative to the plasma flow. Furthermore, we developed an efficient method that can effectively distinguish "magnetic bottle like" and "FRs like" structures. The MP presented in this study is identified as magnetic bottle like type. The mechanism to generate the electron scale magnetic bottle like structure is still unclear, suggesting that new theory needs to be developed to understand such small-scale phenomena.

1. Introduction

Magnetic peaks (MPs), characterized by a sudden enhancement of magnetic strength, have been widely observed in the space plasma. The large amount of previous research indicates that the MP is a very common phenomenon in the terrestrial magnetosheath (e.g., Elphic, 1995; Lucek et al., 1999; Roux et al., 2015; Soucek et al., 2008). Three types of the MPs are often observed in the magnetosheath region: flux transfer events (FTEs), the flux ropes (e.g., Huang et al., 2016; Karimabadi et al., 2014), and mirror mode peaks.

FTEs are structures with a bipolar signature in the magnetic field component normal to the magnetopause, and an enhancement in field strength. It was originally described as the result time variations in the rate of reconnection at the magnetopause by Russell and Elphic (1978) and was followed by an updated description that FTEs are a general observational feature of magnetic reconnection at the magnetopause (e.g., Fear et al., 2008, 2009; Kawano & Russell, 1997; Rijnbeek et al., 1984; Wang et al., 2005, 2006; Zhang et al., 2012). Several models were developed to interpret the generation of the FTEs (e.g., the spatially limited reconnection, Russell & Elphic, 1978; multiple X line reconnection, Lee & Fu, 1985; Raeder, 2006; and single X line reconnection, Scholer, 1988; Southwood et al., 1988). Based on in situ measurements, the morphology of FTEs is often described as flux ropes (FRs) (e.g., Eastwood et al., 2012; Xiao, Pu, Huang, et al., 2004). In the magnetosheath, the field lines of the FTEs are connected to the Earth on one side (e.g., Elphic, 1995; Roux et al., 2015). In some specific situations, the FRs can be regarded as the 3-D version of 2-D magnetic islands (e.g., Fu et al., 2015, 2016) and their spatial size is of the order of a few Earth radii (R_E).

The magnetic mirror mode, a well-known phenomenon in which the field strength is anticorrelated with the plasma density and embedded within the ambient plasma flow, has long been of interest in space physics. Mirror modes are generated by the mirror instability, which is dominantly excited in high ion temperature anisotropy and large plasma beta environments, such as the solar wind and planetary magnetosheath (e.g., Joy et al., 2006; Soucek et al., 2008; Tsurutani et al., 1984; Yao et al., 2013). It is usually characterized by a series of magnetic holes (dips and troughs) and peaks (humps) (e.g., Winterhalter et al., 1994; Xiao et al., 2010, 2011, 2014; Zhang et al., 2008, 2009). From the first theoretical studies of the instability (Tajiri, 1967; Vedenov & Sagdeev, 1958), the importance of mirror mode and its physical effects have been recognized.

Previous studies mainly focus on large-scale mirror mode peaks and the FRs, namely, on the MHD scale. It is noteworthy that there is a counterpart of the mirror mode instability which is so-called "electron mirror instability." It was developed more than three decades ago (Basu & Coppi, 1982, 1984) in a hot electron and cold ion plasma environment. Similar to the mirror mode, this instability is excited by electron anisotropy and described by fluid-like equations (e.g., Basu & Coppi, 1982, 1984; Pokhotelov et al., 2013). Therefore, the instability and its excited structures are still in the MHD scale. In recent Magnetospheric Multiscale (MMS) (Burch et al., 2015) studies, ion scale FRs were observed during the reconnection at the magnetopause (Eastwood et al., 2016). Nonideal ion behavior and filamentary currents were exhibited. Huang et al. (2016) identified this kind of ion scale structure in the turbulent magnetosheath as a magnetic island. Intense wave activities and electron beams were found near the structure.

Due to the low resolution of available data, previous studies have seldom referred to small size magnetic peaks. If ever the word "small" is used, the minimum size is the ion scale. In this study, we report a new kind of electron scale magnetic peak and show new observations of an electron scale physical process. Burst mode MMS data are used, which have 128 Hz sampling for magnetic fields from the Fluxgate Magnetometer (FGM) instrument (Russell et al., 2016), and 150 ms and 30 ms resolution for the ion and electron measurements, respectively, from the Fast Plasma Investigation (FPI) instrument (Pollock et al., 2016). The structure is observed in a spatial scale of ~7 ρ_e (electron gyroradius) or ~0.06 ρ_i (ion gyroradius) and lasted ~0.18 s. The plasma features are detailed in section 2.1. Current densities and electron distributions are analyzed in section 2.2. Three multisatellite techniques are used to determine the morphology, dimensionality, and propagation velocity of the peaks in section 2.3. In section 2.4 we present a simple and reliable method to distinguish "magnetic bottle like" structures (such as magnetic mirror and mirror mode structures) and "FRs like" structures, since they are very similar in space observations. This is followed by a summary and discussion section.

2. Observations

2.1. Plasma Features

Figures 1a–1e show an overview of magnetic field and plasma properties around 11:11:26 UT on 27 January 2017. Figures 1a–1e show the ion and electron energy spectra, three magnetic field components (in geocentric solar ecliptic (GSE) coordinates), and magnetic strength, plasma density, and amplitude of bulk velocity, recorded by MMS1. MMS spacecraft were located at about [9.9,−1.9, 2.1] R_E, and the four spacecraft approximately formed a regular tetrahedron with an average spacecraft separation of ~6 km. MMS1 crossed the magnetopause at~11:11:10 UT (the first dashed line), and remained in magnetosheath until ~11:11:57 UT (the second dashed line). The MP was observed at ~11:11:26.0 UT (in the blue shadow region).

Figures 1f–1q present the details of this MP event. An intense enhancement of magnetic field magnitude is used to identify the magnetic peak (Figure 1f). The scale size of the MP is ~0.06 ρ_i (i.e., ~7 ρ_e), obtained from$(V \times \Delta t)/(\rho_i$ or $\rho_e)$, where V is the averaged background ion bulk velocity (~240 km/s) and Δt is the duration (~0.18 s). The term ρ_i (ρ_e) is the ion (electron) gyroradius, which is ~707 km (~6 km), calculated from 4 nT and 800 eV (96 eV) for this event. The increase in magnetic field strength from ~4 nT to ~14 nT was detected by all four spacecraft (Figure 1f). Figure 1i shows a distinctive variation in the electron flow inside the peak. Strong bipolar signatures in the electron velocity in x and z components and a decrease in the y component are detected. The resolution of the ion data does not allow us to resolve more detailed changes of the ion bulk flows within the MP. Nevertheless, it is expected that the ion bulk flow would not be affected by a MP with such a small-scale size (Eastwood et al., 2016; Huang et al., 2016; Huang, Sahraoui, et al., 2017;

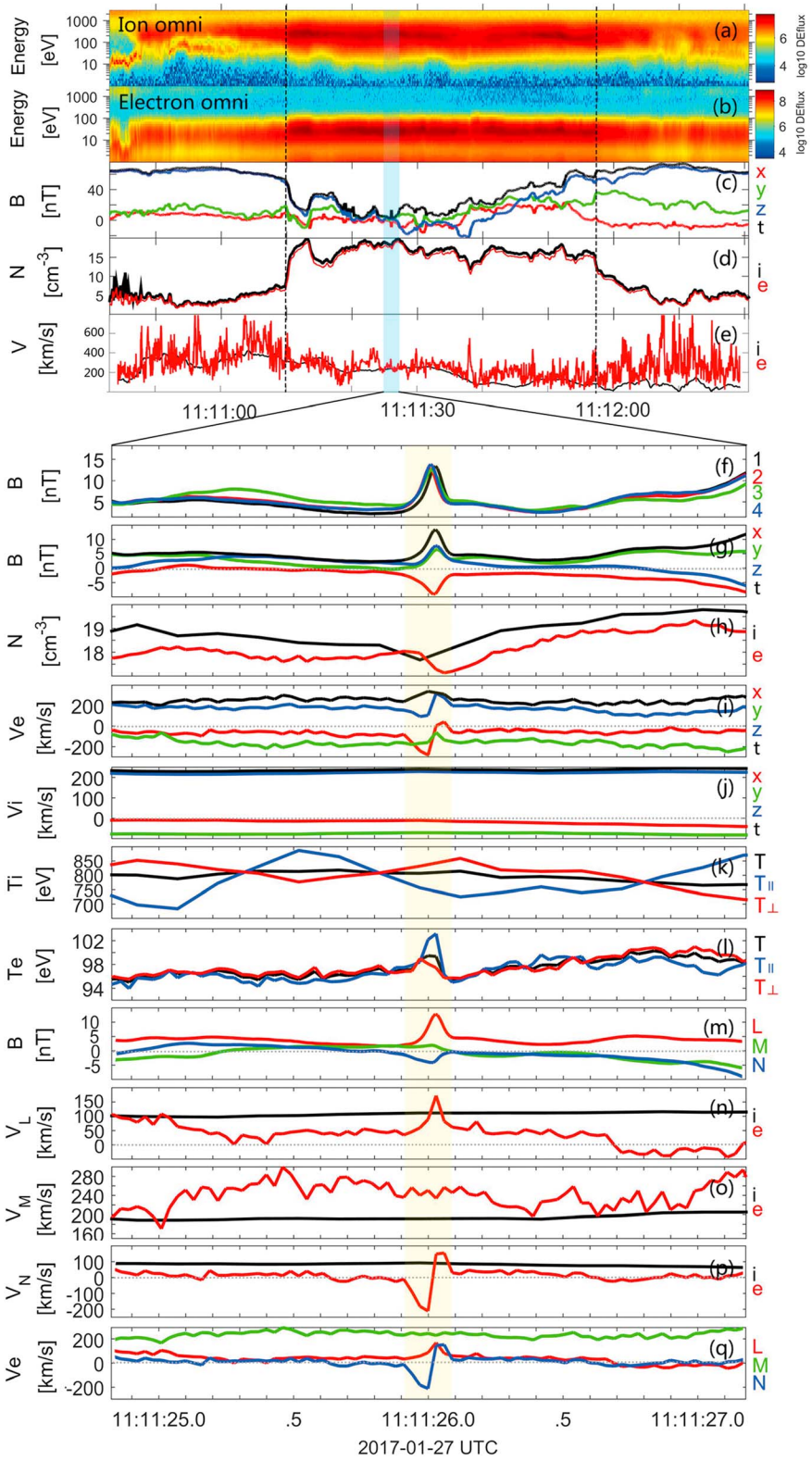

Figure 1. Overview plot of MMS1 observations. (a, b) Ion and electron differential energy fluxes in the omnidirection. (c) Magnetic field strength and components in the GSE coordinate. (d) Ion and electron number density. (e) Ion and electron bulk velocity. Details of the observed MP. (f) Magnetic field magnitude of MMS1–MMS4. MMS1 observations of magnetic field and plasma data. (g) Magnetic field strength and components in the GSE coordinate. (h) Ion and electron number density. (i, j) Ion and electron bulk velocity in the in the GSE coordinate. (k, l) Ion and electron temperature. (m–q) Magnetic field and ion and electron bulk velocity in the LMN coordinate.

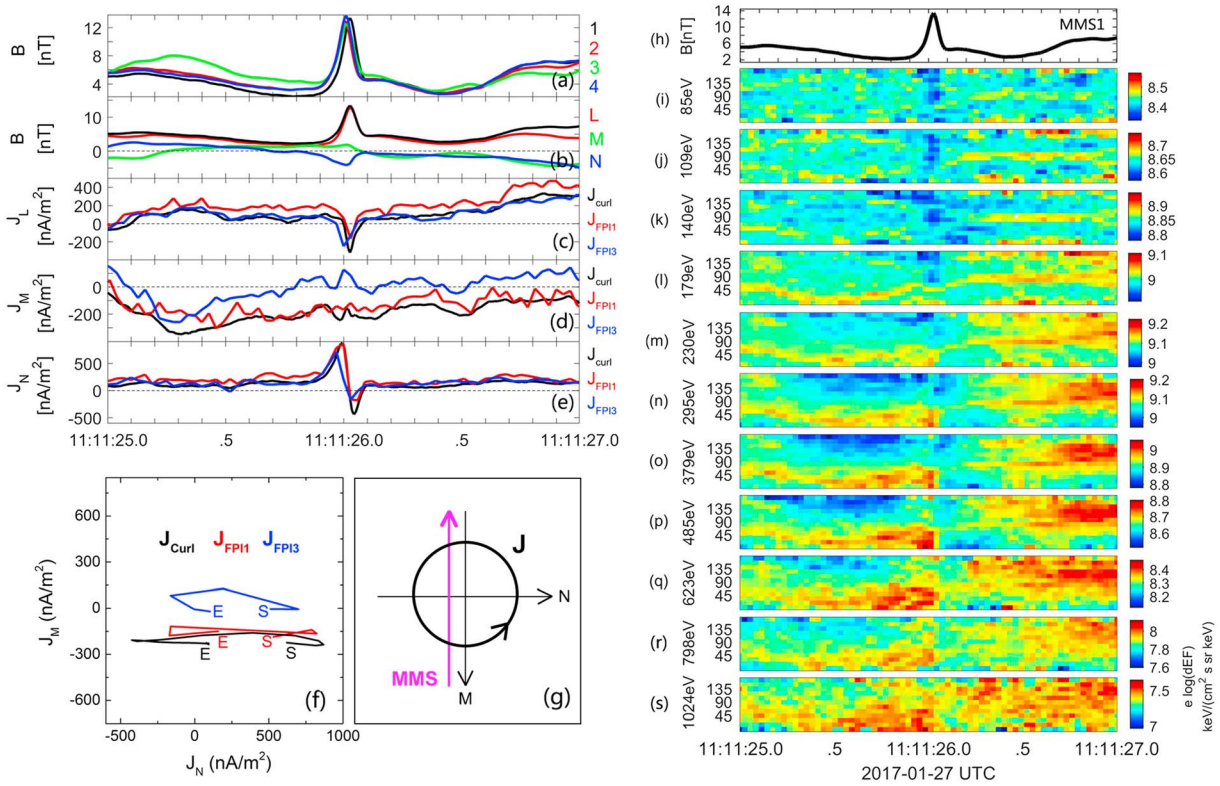

Figure 2. (a) Magnetic field magnitude of MMS1–MMS4. (b) Magnetic field strength and components of MMS1 in the GSE coordinate. (c–e) Currents in the LMN coordinate. (f) The hodograms for the J_M and J_N. "S" denotes "start" and "E" denotes "end." (g) Sketch of the currents. (h) Magnetic field strength of MMS1. (i–r) Electron pitch angle distributions.

Yao, Wang, et al., 2017). The electron temperature is increased inside the MP. This increase is more significant in the parallel direction than the perpendicular direction (Figure 1l).

Figures 1m–1q show the magnetic field and flow velocity in the LMN coordinate system, which is obtained by conjugating the magnetic field minimum variance analysis (MVA) method (Sonnerup & Scheible, 1998) and spatial-temporal difference (STD) method (Shi et al., 2006). The *L* direction is determined as the maximum variation direction of the MVA result, obtained by using the magnetic field data from MMS1, which is [−0.42, 0.62, 0.66] in GSE coordinates. We project the structure propagation velocity (see section 2.3) to the plane perpendicular to *L* direction. The direction of this projection is defined as the *M* direction, which is [−0.24, −0.78, 0.58] in GSE coordinates. The *N* direction, [0.87, 0.09, 0.47], is obtained by completing the right-handed orthogonal coordinate system. Figure 1m shows that the magnetic field is mainly increased along the *L* direction, and the bipolar signatures are along the *M* and *N* directions. When crossing the MP, an electron velocity enhancement is detected in the *L* direction (Figure 1n). Significant electron velocity bipolar variations can be found in the *N* direction (Figure 1p), implying the existence of electron vortex in the *M*-*N* plane.

2.2. Current Density and Electron Distributions

The current density can be calculated using the Curlometer method (Dunlop et al., 2002). The results are displayed in Figures 2c–2e (J_{Curl}, black line). The current density is also estimated from particle moments: $J_{FPI} = n_e e(v_i - v_e)$, where n_e is the electron number density, v_i, v_e are the ion and electron bulk velocities, and e is the elementary coulomb charge. The peak value of magnetic strength from MMS1 is maximum, and the peak value from MMS3 is minimum, so the calculated currents from MMS1-FPI (J_{FPI1}) and MMS3-FPI (J_{FPI3}) are plotted to compare with the current calculated from Curlometer method, and they are found to be consistent with each other. The plasma bulk velocities in Figures 1n–1p show that ion flows are nearly unchanged when crossing the MP. The current is dominantly caused by the variation of electron flows. Intense currents show a strong axial component (*L* direction). Significant bipolar variations of J_{Curl}, J_{FPI1},

and J_{FPI3} are detected in the *N* direction while slight fluctuations are observed in the *M* direction. This implies that an electron vortex is in the *M-N* plane and is self-consistent with the increased magnetic strength in the *L* direction. Figure 2f shows the hodograms for J_{Curl}, J_{FPI1}, and J_{FPI3}. The current densities in the *M* and *N* directions constitute a "straight line" shape for J_{FPI1} and an "irregular ellipse" shape for J_{FPI3}. For a trajectory (along the negative *M* direction) across the center of ideal vortex, only the current density perpendicular to the *M* direction should vary, while for a trajectory not across the center, the current density should vary both in the M and N directions. Thus, we speculate that the trajectory of MMS1 is close to the vortex center, whereas the trajectory of MMS3 is farther away. This deduction can also be verified by the magnetic field data, namely, the amplitude of the peak is largest for MMS1 and is smallest for MMS3. A sketch of the current is plotted in Figure 2g. The current density along the trajectory changes from positive to negative in the *N* direction. In the *M* direction, it has a maximum when nearest to the center. Furthermore, in Figure 2g, the magnetic field deduced from the current is along the *L* direction. These fit well with the observations. Figures 2i–2s show the electron pitch angle distributions (PADs) of MMS1. Electron fluxes increase at near 0° from 179 eV to 1024 eV (Figures 2i–2s), indicate the observations of electron beams, and behave as the increase of electron parallel temperature (Figure 1l). The electron energy fluxes from 85 eV to 140 eV decreased in all directions. For electrons with energies from 179 eV to 1024 eV, it is unclear whether a decreasing trend persists due to the coexistence of parallel electron beams. Note that in this case, we find electron beams within the structure, which is typically a feature of a sheath boundary layer in which field lines have one side connected with the Earth under northward IMF conditions (e.g., Lavraud et al., 2005; Onsager et al., 2001). Further research will be carried out to investigate whether electron scale MPs of the kind reported here are more or less likely to occur within the sheath boundary layer.

2.3. Dimensionality and Propagating Velocity

The four spacecraft maintained a good tetrahedron shape when crossing the MP, and the averaging spacecraft separation is several times smaller than the size of the MP. This situation is suitable to use the minimum directional derivative (MDD) method (Shi et al., 2005, 2013; Shi, Pu, et al., 2009; Shi, Zong, et al., 2009) and STD method to determine the dimensionality and propagation velocity of the MP. With the MDD method, the dimensionality of the structure can be obtained and it provides maximum, minimum, and intermediate variations of the observed field, labeled λ_1, λ_2, and λ_3, respectively, and shown in Figure 3b. From Figure 3b we can find $\lambda_1 \gg \lambda_2 \gg \lambda_3$ in the two edges, which shows a transition between 1-D (flattened tube) and 2-D (circular tube), inferring that the MP is of the ellipse shape. The STD method can calculate the propagation velocity of quasi-stationary structures if we deem the MP as 1-D, as shown in Figure 3d.

Figure 3c shows the magnetic field maximum variation direction $\overrightarrow{n}$ in the time series. The vector $\overrightarrow{n}$ (0.05, −0.95, 0.30) averaged in the leading edge (red region) and trailing edge (blue regions) are considered as the propagating direction of the MP. The average propagating velocity *U* in the satellite frame is ~210 km/s along $\overrightarrow{n}$ (Figure 3d). The background ion flow $\overrightarrow{V}$ is about (−20.3, −77.7, 221.5) km/s. Therefore, the propagation velocity in the ion flow frame is obtained as $V_P = U - \overrightarrow{V}\cdot\overrightarrow{n} = 70.8\pm5.6$ km/s. As we know, mirror mode structures are non-propagating in space plasmas (e.g., Hasegawa, 1969; Southwood & Kivelson, 1993). Therefore, the MP is clearly different from the mirror mode structures. Here we consider the ion flow as the background plasma flow since it is much quieter than the electron flow. In electron flow frame, we find the MP may nonpropagate (for more details, please see the supporting information). Figure 3e shows that the ratio between the computed divergence and the curl of the magnetic field is much less than 0.2, indicating the results are credible (Dunlop et al., 1990; Robert et al., 1998; Xiao, Pu, Ma, et al., 2004). To compare with MDD and STD method, Figures 3f and 3g show the results of *U* and $\overrightarrow{n}$ calculated by the timing method (see Paschmann et al., 1998; Russell et al., 1983). Four timing calculations are done. The distances and time intervals of the calculations are obtained from the data of four satellites when the magnetic field magnitude is equal to a given value. The given values are 8, 9, 10, and 11 nT, which corresponding to four timing calculations presented as black, blue, red, and green horizontal lines in Figure 3a, respectively. Since we consider an uncertain (see the details of Xiao et al., 2014, and Yao et al., 2016, and reference therein), the results are presented as distributions in Figures 3f and 3g, and the standard deviations of the distributions are considered as the errors of the results. It can be seen that the timing results (e.g., for the calculation when magnetic field magnitude is 9 nT in leading boundary, $U_2 = 240.4 \pm 14.5$ km/s, $n_2 = [0.00, -0.94, 0.31] \pm 0.7°$) agree well with that of the MDD and STD methods.

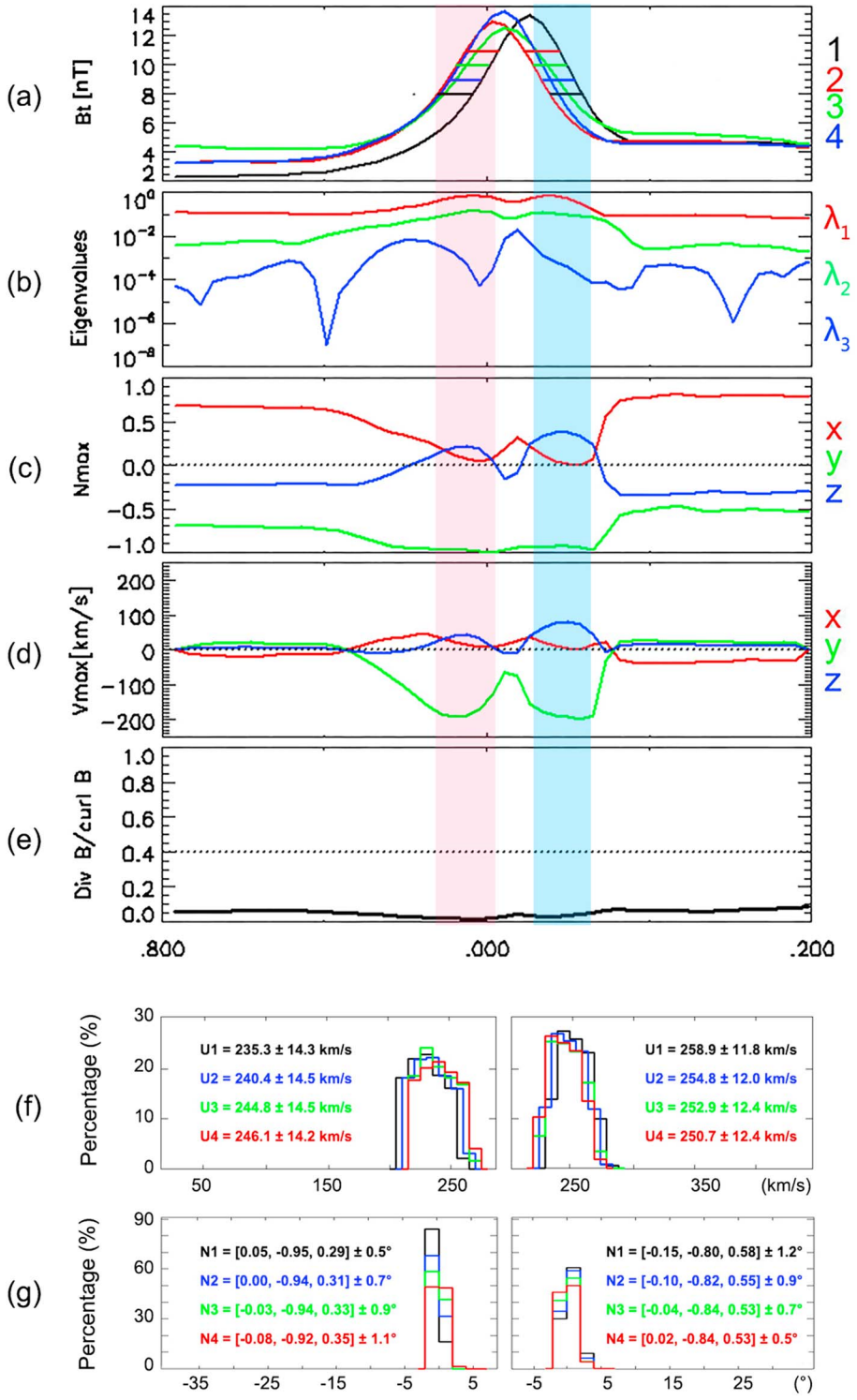

Figure 3. (a) Magnetic field magnitude of MMS1–MMS4. Four horizontal lines represent four timing calculations. The red and blue regions correspond to the leading and trailing edges of the MP, respectively. Dimensionality and velocity calculated from MDD and STD methods (Shi et al., 2005, 2006). (b) Eigenvalues λ_1, λ_2, and λ_3. (c) Magnetic field maximum derivative direction calculated at every moment. (d) Velocity along the maximum derivative direction. (e) The ratio between the divergence and the curl of the magnetic field, used for measuring the credibility results of the MDD and STD methods. (f–g) Timing results of the velocity and normal for leading edge (left column) and trailing edge (right column) in distribution type. Four colors correspond to the four timing calculations in Figure 3a.

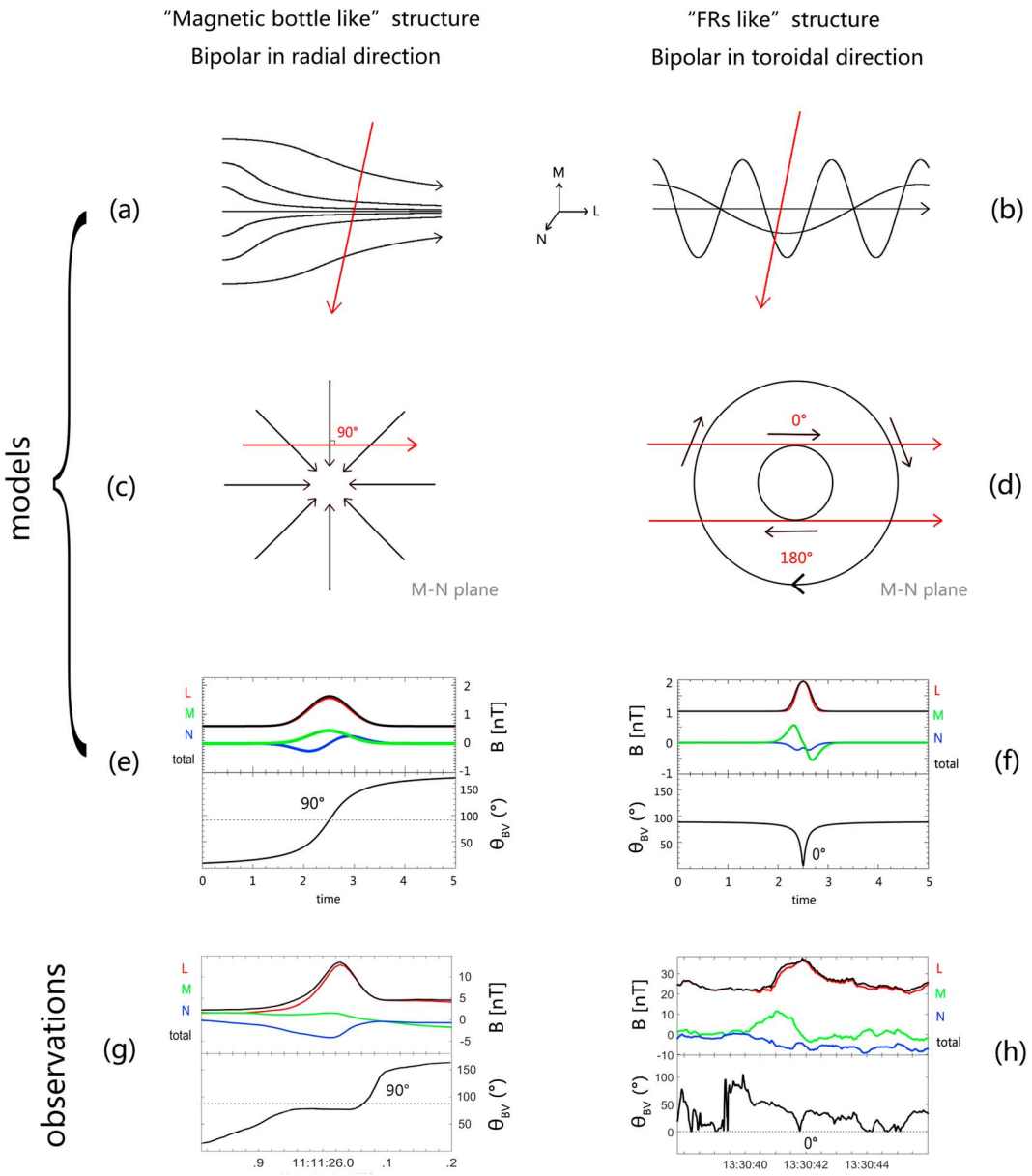

Figure 4. (a, b) Models of the magnetic bottle like (Tao, 2014) and FRs like (Elphic & Russell, 1983) structures. Magnetic field lines and satellites trajectories are denote as the black and red lines, respectively. (c, d) The crossing in the *M-N* plane for models. (e, f) Observational features along the trajectories for models. (g, h) Two observed magnetic peaks corresponding to the magnetic bottle like and FRs like structures.

2.4. A Method to Distinguish the Magnetic Bottle Like and the FRs Like Structures

A bipolar signal in the magnetic field is usually used to identify FRs in space, while, in general, the magnetic component along the axis has an enhanced signal when crossing a flux rope. However, in a certain cases, magnetic bottle like structures, such as the mirror mode structure and magnetic mirror, share similar observational signals with flux rope structures. Figure 4 shows the similarities and differences in observations between these two types of MP structures. Figures 4a and 4b show three dimensional models for the "magnetic bottle like structure" (adopted from Tao, 2014) and the flux rope (adopted from Elphic & Russell, 1983), respectively (see supporting information). The magnetic field lines are shown as black curves. The spacecraft trajectories are represented by red lines. The *L* directions in both cases are along the axis of the structures. Figures 4c and 4d show cuts in the *M-N* plane when crossing the models. Figures 4e and 4f show observational features along the trajectories for the models. The magnetic field strengths are enhanced and bipolar signatures in the MN plane are observed for both two structures.

There is, however, a distinct difference between the two structures. For the magnetic bottle like structure, the field lines in the *MN* plane are radially inward (or outward), and the angle (θ_{BV}) between the field line and the spacecraft trajectory is equal to 90° when the spacecraft passes the point of closest approach to the structure center (Figure 4e). On the contrary, the field lines of the FRs like structure have toroidal features, and an angle equal to 180° or 0° will be obtained as the center of the flux rope is passed (Figure 4f). Figure 4g shows the angle calculated for the MP in this study, while Figure 4h shows a flux rope case observed on 11 October 2015. In Figure 4h, the angle is nearly 0° at the center of the peak, implying that it is a FRs like (toroidal direction field) structure. Figure 4g clearly shows that the angle is approaching to 90° near the center of the peak, implying the MP studied in this paper is magnetic bottle like (radial direction field). In addition, we have applied this method to the cases in Zhang et al. (2012), Guo et al. (2016), and Huang et al. (2016), and all the results are consistent with the previous studies (not shown). Of the 205 kinetic scale MPs observed in the magnetosheath (with temporal scales $<$1.5 s, observed from September 2015 to February 2016 and from October 2016 to January 2017), 44 cases have similar features with the case observed in this study. Ninety cases are unclear and the rest are identified as flux ropes. More detailed statistical analysis will be carried out in the near future.

3. Summary and Discussions

3.1. Summary of the Observations

In this study, we report a new type of electron scale MP in the magnetosheath. The scale size of the MP is ~7 ρ_e or ~0.06 ρ_i and the duration is ~0.18 s. Enhanced magnetic field and current density are detected in the field aligned direction. Electron vortex is found perpendicular to the field lines and the current system is consistent with the magnetic peak. Several multipoint spacecraft techniques are used to determine the propagation velocity. It is found that the MP is propagating in the plasma (ion) flow. Furthermore, we developed an efficient method that can effectively distinguish between magnetic bottle like and FRs like structures. We have also tested the method on previously well-studied events, and found good consistency with all those examples. The MP in this study is identified as magnetic bottle like structure. In previous studies, the low data resolution limits the development of kinetic scale physics. This study shows distinct observations of a new kind of electron scale magnetic peak and provides new reference not only on the observations of space physics, but also on the related basic plasma theories and numerical simulations. Their associated unsettled questions, e.g., plasma instability and dissipation in turbulence, can be widely studied.

3.2. Discussions

The scale size of the peak in this work is obtained from ($V \times dt$)/(ρ_i or ρ_e), and the ρ_i and ρ_e are 707 km and 6 km, respectively. They are larger than the typical magnetosheath ρ_i (50–100 km) and ρ_e (0.5–1 km) since the background magnetic field of the peak (~4 nT) is lower and the temperatures (805 eV for ions and 96 eV for electrons) are higher than typically the case in the magnetosheath. This provides an opportunity to study a rather small size (namely, 0.06 ρ_i or 7 ρ_e) MP under the particle gyroradius scale. In previously studies, this kind of electron scale structure cannot be detected or well investigated due to the limitations of the satellite data resolution. Since the launch of MMS, we have the chance to study kinetic scale structures through the high time resolution data. Several studies on ion scale MPs have been carried out, which are all FRs (e.g., Eastwood et al., 2016; Huang et al., 2016). Eastwood et al. (2016) and Huang et al. (2016) investigated a kind of ion scale FRs with the scale size of 10–20 ρ_i (1,100 km) and 6 ρ_i (240 km) respectively, which are hundreds of times greater than the size of the peak in this study. For the structures with the scale size close to ρ_i and much larger than ρ_e, electrons are therefore coupled to magnetic field lines while ions are partially or entirely decoupled. The ions may not respond to the structure and are regarded as the background. Since the physical process is electron dynamics dominated, electron magnetohydrodynamics (EMHD) may be appropriate for these structures (e.g., Yao, Wang, et al., 2017; Yao, Rae, et al., 2017).

In section 2.4, the MP is identified as magnetic bottle like rather than FRs like structure. We can exclude that the MP is the swing of the magnetopause, based on the fact that the structure can be observed by all four spacecraft in the same order (e.g., Shi, Pu, et al., 2009). The MPs in the terrestrial magnetosheath are usually mirror mode peaks and FRs. The mirror mode structures in previous studies are generally in MHD scale rather than kinetic scale. The general mirror mode structure is excited by the mirror instability in an anisotropic hot

ion environment and can exist in the mirror stable environment. The scale size of the peak in this study is close to ρ_e. The generation mechanism in the MHD framework may be not appropriate for it. Previous studies indicate that the mirror mode is nonpropagating in the plasma flow (e.g., Hasegawa, 1969; Southwood & Kivelson, 1993). However, as we have demonstrated in section 2.3, the peak was propagating in the background ion plasma, which strongly implies a different generation mechanism. One possible scenario is that the mirror mode peak drifts in the plasma caused by gradient of magnetic field and density (drift mirror mode, Hasegawa, 1969) and propagates into low-intensity magnetic strength regions. The ions escaped due to their larger gyroradius. Hence, the structure is declining and contracting, which in turn allows more ions to escape. Finally, the ions are not coupled to the structure and the electron dynamic process dominates. Another possible generation mechanism is that the structure is excited by some electron instability. Figures 1l, 2c and 2i–2s show the existence of parallel electron beams. Some electron instability related to the electron beams may be excited.

It is worth discussing the relation between the MP in this paper and kinetic scale magnetic holes (KSMHs). In recent MMS discoveries, Yao, Wang, et al. (2017) shows a series of KSMHs with a scale size of 10–20 ρ_e in the magnetosheath. Those observations show diamagnetic electron vortices in the plane perpendicular to the magnetic field. Huang, Du, et al. (2017) also statistically investigated KSMHs in the turbulent magnetosheath (Huang, Hadid, et al., 2017). Those KSMHs contain electron vortices similar to the MP and their scale size is tens or several tens of ρ_e, close to the MP scale. Actually, the KSMHs are observed not only in the magnetosheath but also in the plasma sheet (Ge et al., 2011; Gershman et al., 2016; Sun et al., 2012; Sundberg et al., 2015; Yao et al., 2016; Zhang et al., 2017). The KSMHs in the plasma sheet are also of similar scale size to the MP. Furthermore, these observations display a depolarized magnetic field (Ge et al., 2011), an electron vortex (Gershman et al., 2016; Zhang et al., 2017), and propagation with respect to the plasma flow (Yao et al., 2016), analogous to the properties of the MP. Thus, we speculate that the MP and the KSMHs could be intrinsically linked. In a recent particle-in-cell (PIC) simulation, KSMHs within a decaying turbulence are reported by Haynes et al. (2015). This study shows diamagnetic azimuthal current associated with the magnetic field depression. The study also implies a relation between turbulence and kinetic scale magnetic structure. As we know, in the turbulent plasma (e.g., the solar wind and magnetosheath), the magnetic energy spectra exhibit several dynamical ranges. The dissipation range (e.g., Goldstein et al., 1994) is near ion scales, and the dispersive range (e.g., Alexandrova et al., 2012; Breuillard et al., 2016; Huang et al., 2014; Sahraoui et al., 2006, 2013) is far below the ion scale. In these ranges, dissipation, dispersion, and kinetic effects become important. Thus, these kinetic scale structures (typically not to mention the electron scale MP reported in this study and the KSMHs in recent studies) may play important roles in transporting particles and dissipating energy in turbulent plasmas. Further, detailed comparison between the theories, simulations, and satellite observation results are to be performed in our future research.

Acknowledgments
The instrumental teams of MMS are greatly appreciated for providing magnetic field and plasma data. MMS data are available from MMS Science Data Center (https://lasp.colorado.edu/mms/sdc/public/). This work was supported by the National Natural Science Foundation of China (grants 41774153, 41574157, and 41628402) and the young scholar plan of Shandong University at Weihai (2017WHWLJH08). Z. Y. is a Marie-Curie COFUND postdoctoral fellow at the University of Liege. Co-funded by the European Union. HZ is partially supported by NSF AGS-1352669.

References

Alexandrova, O., Lacombe, C., Mangeney, A., Grappin, R., & Maksimovic, M. (2012). Solar wind turbulent spectrum at plasma kinetic scales. *Astrophysical Journal*, *760*(2), 2680–2700.

Basu, B., & Coppi, B. (1982). Field-swelling instability in anisotropic plasmas. *Physical Review Letters*, *48*, 799.

Basu, B., & Coppi, B. (1984). Theory of field-swelling instability in anisotropic plasmas. *Physics of Fluids*, *27*, 1187–1193. https://doi.org/10.1063/1.864725

Breuillard, H., Yordanova, E., Vaivads, A., & Alexandrova, O. (2016). The effects of kinetic instabilities on small-scale turbulence in earth's magnetosheath. *The Astronomical Journal*, *829*(1), 54. https://doi.org/10.3847/0004-637X/829/1/54

Burch, J. L., Moore, T. E., Torbert, R. B., & Giles, B. L. (2015). Magnetospheric multiscale overview and science objectives. *Space Science Reviews*, *199*, 1–17. https://doi.org/10.1007/s11214-015-0164-9

Dunlop, M. W., Balogh, A., Southwood, D. J., Elphic, R. C., Glassmeier, K.-H., & Neubauer, F. M. (1990). Configuration sensitivity of multipoint magnetic field measurements. In *Proceedings of the International Workshop on Space Plasma Physics Investigations by Cluster Regatta* (pp. 23–28). ESA SP-306. Paris, France: European Space Agency.

Dunlop, M. W., Balogh, A., Glassmeier, K.-H., & Robert, P. (2002). Four-point Cluster application of magnetic field analysis tools: Thecurlometer. *Journal of Geophysical Research*, *107*(A11), 1384. https://doi.org/10.1029/2001JA005088

Eastwood, J. P., Phan, T. D., Fear, R. C., Sibeck, D. G., Angelopoulos, V., Oieroset, M., & Shay, M. A. (2012). Survival of flux transfer event (FTE) flux ropes far along the tail magnetopause. *Journal of Geophysical Research*, *117*, A08222. https://doi.org/10.1029/2012JA017722

Eastwood, J. P., Phan, T. D., Cassak, P. A., Gershman, D. J., Haggerty, C., Malakit, K., … Wang, S. (2016). Ion-scale secondary flux ropes generated by magnetopause reconnection as resolved by MMS. *Geophysical Research Letters*, *43*, 4716–4724. https://doi.org/10.1002/2016GL068747

Elphic, R. C. (1995). Observations of flux transfer events: A review. In P. Song, B. U. Ö. Sonnerup, & M. F. Thomsen (Eds.), *Physics of the magnetopause*, *Geophysical Monograph Series*, (Vol. 90, pp. 225–233). Washington, DC: American Geophysical Union.

Elphic, R. C., & Russell, C. T. (1983). Magnetic flux ropes in the Venus ionosphere: Observations and models. *Journal of Geophysical Research*, *88*(A1), 58–72. https://doi.org/10.1029/JA088iA01p00058

Fear, R. C., Milan, S. E., Fazakerley, A. N., Lucek, E. A., Cowley, S. W. H., & Dandouras, I. (2008). The azimuthal extent of three flux transfer events. *Annales de Geophysique*, *26*(8), 2353–2369. https://doi.org/10.5194/angeo-26-2353-2008

Fear, R. C., Milan, S. E., Fazakerley, A. N., Fornacon, K.-H., Carr, C. M., & Dandouras, I. (2009). Simultaneous observations of flux transfer events by THEMIS, Cluster, Double Star and SuperDARN: Acceleration of FTEs. *Journal of Geophysical Research*, *114*, A10213. https://doi.org/10.1029/12009JA014310

Fu, H. S., Vaivads, A., Khotyaintsev, Y. V., Olshevsky, V., André, M., Cao, J. B., … Lapenta, G. (2015). How to find magnetic nulls and reconstruct field topology with MMS data? *Journal of Geophysical Research: Space Physics*, *120*, 3758–3782. https://doi.org/10.1002/2015JA021082

Fu, H. S., Cao, J. B., Vaivads, A., Khotyaintsev, Y. V., Andre, M., Dunlop, M., … Eriksson, E. (2016). Identifying magnetic reconnection events using the FOTE method. *Journal of Geophysical Research: Space Physics*, *121*, 1263–1272. https://doi.org/10.1002/2015JA021701

Ge, Y. S., McFadden, J. P., Raeder, J., Angelopoulos, V., Larson, D., & Constantinescu, O. D. (2011). Case studies of mirror-mode structures observed by THEMIS in the near-Earth tail during substorms. *Journal of Geophysical Research*, *116*, A01209. https://doi.org/ 10.1029/2010JA015546

Gershman, D. J., Dorelli, J. C., Viñas, A. F., Avanov, L. A., Gliese, U., Barrie, A. C., … Burch, J. L. (2016). Electron dynamics in a subproton-gyroscale magnetic hole. *Geophysical Research Letters*, *43*, 4112–4118. https://doi.org/10.1002/2016GL068545

Goldstein, M. L., Roberts, D. A., & Fitch, C. A. (1994). Properties of the fluctuating magnetic helicity in the inertial and dissipation ranges of solar wind turbulence. *Journal of Geophysical Research*, *99*(A6), 11519–11538. https://doi.org/10.1029/94JA00789

Guo, R., Pu, Z., Chen, L. J., Fu, S., Xie, L., Wang, X., … Fazakerley, A. N. (2016). In-situ observations of flux ropes formed in association with a pair of spiral nulls in magnetotail plasmas. *Physics of Plasmas*, *23*(5), 478–144.

Hasegawa, A. (1969). Drift mirror instability in the magnetosphere. *Physics of Fluids*, *12*(12), 2642–2650. https://doi.org/10.1063/1.1692407

Haynes, C. T., Burgess, D., Camporeale, E., & Sundberg, T. (2015). Electron vortex magnetic holes: A nonlinear coherent plasma structure. *Physics of Plasmas*, *22*(1), 012309. https://doi.org/10.1063/1.4906356

Huang, S. Y., Sahraoui, F., Deng, X. H., He, J. S., Yuan, Z. G., Zhou, M., … Fu, H. S. (2014). Kinetic turbulence in the terrestrial magnetosheath: Cluster observations. *The Astrophysical Journal Letters*, *789*(2), L28. https://doi.org/10.1088/2041-8205/789/2/L28

Huang, S. Y., Sahraoui, F., Retino, A., le Contel, O., Yuan, Z. G., Chasapis, A., … Burch, J. L. (2016). MMS observations of ion-scale magnetic island in the magnetosheath turbulent plasma. *Geophysical Research Letters*, *43*, 7850–7858. https://doi.org/10.1002/2016GL070033

Huang, S. Y., Sahraoui, F., Yuan, Z. G., He, J. S., Zhao, J. S., Contel, O. L., … Burch, J. L. (2017). Magnetospheric multiscale observations of electron vortex magnetic hole in the magnetosheath turbulent plasma. *Astrophysical Journal*, *836*(2). https://doi.org/10.3847/2041-8213/aa5f50

Huang, S. Y., Hadid, L. Z., Sahraoui, F., Yuan, Z. G., & Deng, X. H. (2017). On the existence of the Kolmogorov inertial range in the terrestrial magnetosheath turbulence. *The Astrophysical Journal Letters*, *836*, L10. https://doi.org/10.3847/2041-8213/836/1/L10

Huang, S. Y., Du, J. W., Sahraoui, F., Yuan, Z. G., He, J. S., Zhao, J. S., … Burch, J. L. (2017). A statistical study of kinetic-size magnetic holes in turbulent magnetosheath: MMS observations. *Journal of Geophysical Research: Space Physics*, *122*, 8577–8588. https://doi.org/10.1002/2017JA024415

Joy, S. P., Kivelson, M. G., Walker, R. J., Khurana, K. K., Russell, C. T., & Paterson, W. R. (2006). Mirror-mode structures in the Jovian magnetosheath. *Journal of Geophysical Research*, *111*, A12212. https://doi.org/10.1029/2006JA011985

Karimabadi, H., Roytershteyn, V., Vu, H. X., Omelchenko, Y. A., Scudder, J., Daughton, W., … Geveci, B. (2014). The link between shocks, turbulence, and magnetic reconnection in collisionless plasmas. *Physics of Plasmas*, *21*(6), 062308. https://doi.org/10.1063/1.4882875

Kawano, H., & Russell, C. T. (1997). Survey of flux transfer events observed with the ISEE 1 spacecraft: Dependence on the interplanetary-magnetic field. *Journal of Geophysical Research*, *102*(A6), 11,307–11,313. https://doi.org/10.1029/97JA00481

Lavraud, B., Thomsen, M. F., Taylor, M. G. G. T., Wang, Y. L., Phan, T. D., Schwartz, S. J., … Balogh, A. (2005). Characteristics of the magnetosheath electron boundary layer under northward interplanetary magnetic field: Implications for high-latitude reconnection. *Journal of Geophysical Research*, *110*, A06209. https://doi.org/10.1029/2004JA010808

Lee, L. C., & Fu, Z. F. (1985). Atheoryofmagneticflux transfer at the Earth's magnetopause. *Geophysical Research Letters*, *12*, 105–108. https://doi.org/10.1029/GL012i002p00105

Lucek, E. A., Dunlop, M. W., Balogh, A., Cargill, P., Baumjohann, W., Georgescu, E., … Fornacon, K.-H. (1999). Mirror mode structures observed in the dawn-side magnetosheath by Equator-S. *Geophysical Research Letters*, *26*(14), 2159–2162. https://doi.org/10.1029/1999GL900490

Onsager, T. G., Scudder, J. D., Lockwood, M., & Russell, C. T. (2001). Reconnection at the high latitude magnetopause during northward interplanetary magnetic field conditions. *Journal of Geophysical Research*, *106*(A11), 25,467–25,488. https://doi.org/10.1029/2000JA000444

Paschmann, G., Fazakerley, A. N., & Schwartz, S. J. (1998). Moments of plasma velocity distributions. In *Analysis methods for multi-spacecraft data*, (pp. 125–158). Noordwijk, Netherlands: ISSI SA Publications Division.

Pokhotelov, O. A., Onishchenko, O. G., & Stenflo, L. (2013). Physical mechanisms for electron mirror and field swelling modes. *Physica Scripta*, *87*(6), 065303. https://doi.org/10.1088/0031-8949/87/06/065303

Pollock, C., Moore, T., Jacques, A., Burch, J., Gliese, U., Saito, Y., … Zeuch, M. (2016). Fast plasma investigation for magnetospheric multiscale. *Space Science Reviews*, *199*(1-4), 331–406. https://doi.org/10.1007/s11214-016-0245-4

Raeder, J. (2006). Flux transfer events: 1. Generation mechanism for strong southward IMF. *Annales de Geophysique*, *24*(1), 381–392. https://doi.org/10.5194/angeo-24-381-2006

Rijnbeek, R. P., Cowley, S. W. H., Southwood, D. J., & Russell, C. T. (1984). A survey of dayside flux transfer events observed by ISEE 1 and 2magnetometers. *Journal of Geophysical Research*, *89*(A2), 786–800. https://doi.org/10.1029/JA089iA02p00786

Robert, P., Dunlop, M. W., Roux, A., & Elphic, R. C. (1998). Accuracy of current density determination. In G. Paschmann & P. W. Daly (Eds.), *Analysis methods for multi-spacecraft data* (pp. 395–418). Paris: European Space Agency.

Roux, A., Robert, P., Fontaine, D., Le Contel, O., Canu, P., & Louarn, P. (2015). What is the nature of magnetosheath FTEs? *Journal of Geophysical Research: Space Physics*, *120*, 4576–4595. https://doi.org/10.1002/2015JA020983

Russell, C. T., & Elphic, R. C. (1978). Initial ISEE magnetometer results: Magnetopause observations. *Space Science Reviews*, *22*, 681–715.

Russell, C. T., Mellott, M. M., Smith, E. J., & King, J. H. (1983). Multiple spacecraft observations of interplanetary shocks: Four spacecraft determinations of shock normals. *Journal of Geophysical Research*, *88*(A6), 4739–4748. https://doi.org/10.1029/JA088iA06p04739

Russell, C. T., Riedler, W., Schwingenshuh, K., & Yeroshenko, Y. (1987). Mirror instability in the magnetosphere of Comet Halley. *Geophysical Research Letters*, *14*(6), 644–647. https://doi.org/10.1029/GL014i006p00644

Russell, C. T., Anderson, B. J., Baumjohann, W., Bromund, K. R., Dearborn, D., Fischer, D., … Richter, I. (2016). The Magnetospheric Multiscale magnetometers. *Space Science Reviews*, *199*(1-4), 189–256. https://doi.org/10.1007/s11214-014-0057-3

Sahraoui, F., Belmont, G., Rezeau, L., & Cornilleau-Wehrlin, N. (2006). Anisotropic turbulent spectra in the terrestrial magnetosheath as seen by the Cluster spacecraft. *Physical Review Letters*, *96*(7), 075002. https://doi.org/10.1103/PhysRevLett.96.075002

Sahraoui, F., Huang, S. Y., Belmont, G., Goldstein, M. L., Retinò, A., Robert, P., & de Patoul, J. (2013). Scaling of the electron dissipation range of solar wind turbulence. *The Astrophysical Journal*, *777*(1), 15. https://doi.org/10.1088/0004-637X/777/1/15

Scholer, M. (1988). Magnetic flux transfer at the magnetopause based on single X-line bursty reconnection. *Geophysical Research Letters*, *15*(4), 291–294. https://doi.org/10.1029/GL015i004p00291

Shi, Q. Q., Shen, C., Pu, Z. Y., Dunlop, M. W., Zong, Q.-G., Zhang, H., … Balogh, A. (2005). Dimensional analysis of observed structures using multipoint magnetic field measurements: Application to Cluster. *Geophysical Research Letters*, *32*, L12105. https://doi.org/10.1029/2005GL022454

Shi, Q. Q., Shen, C., Dunlop, M. W., Pu, Z. Y., Zong, Q.-G., Liu, Z. X., … Balogh, A. (2006). Motion of observed structures calculated from multi-point magnetic field measurements: Application to cluster. *Geophysical Research Letters*, *33*, L08109. https://doi.org/10.1029/2005GL025073

Shi, Q. Q., Pu, Z. Y., Soucek, J., Zong, Q. G., Fu, S. Y., Xie, L., … Reme, H. (2009). Spatial structures of magnetic depression in the Earth's high-altitude cusp: Cluster multipoint observations. *Journal of Geophysical Research*, *114*, A10202. https://doi.org/10.1029/2009JA014283

Shi, Q. Q., Zong, Q. G., Zhang, H., Pu, Z. Y., Fu, S. Y., Xie, L., … Lucek, E. (2009). Cluster observations of the entry layer equatorward of the cusp under northward interplanetary magnetic field. *Journal of Geophysical Research*, *114*, A12219. https://doi.org/10.1029/2009JA014475

Shi, Q. Q., Zong, Q. G., Fu, S. Y., Dunlop, M. W., Pu, Z. Y., Parks, G. K., … Lucek, E. (2013). Solar wind entry into the high-latitude terrestrial magnetosphere during geomagnetically quiet times. *Nature Communications*, *4*, 1466. https://doi.org/10.1038/ncomms2476

Sonnerup, B. U. O., & Scheible, M. (1998). Minimum and maximum variance analysis. In G. Paschmann & P. W. Daly (Eds.), *Analysis methods for multi-spacecraft data* (pp. 185–220). Bern: European Space Agency.

Soucek, J., Lucek, E., & Dandouras, I. (2008). Properties of magnetosheath mirror modes observed by Cluster and their response to changes in plasma parameters. *Journal of Geophysical Research*, *113*, A04203. https://doi.org/10.1029/2007JA012649

Southwood, D. J., & Kivelson, M. G. (1993). Mirror instability: 1. Physical mechanism of linear instability. *Journal of Geophysical Research*, *98*(A6), 9181–9187. https://doi.org/10.1029/92JA02837

Southwood, D. J., Farrugia, C. J., & Saunders, M. A. (1988). What are flux transfer events? *Planetary and Space Science*, *36*, 503–508.

Sun, W. J., Shi, Q. Q., Fu, S. Y., Pu, Z. Y., Dunlop, M. W., Walsh, A. P., … Fazakerley, A. (2012). Cluster and TC-1 observation of magnetic holes in the plasma sheet. *Annals of Geophysics*, *30*(3), 583–595. https://doi.org/10.5194/angeo-30-583-2012

Sundberg, T., Burgess, D., & Haynes, C. T. (2015). Properties and origin of subproton-scale magnetic holes in the terrestrial plasma sheet. *Journal of Geophysical Research: Space Physics*, *120*, 2600–2615. https://doi.org/10.1002/2014JA020856

Tajiri, M. (1967). Propagation of hydromagnetic waves in collisionless plasma, II, Kinetic approach. *Journal of the Physical Society of Japan*, *22*, 1482.

Tao, X. (2014). A numerical study of chorus generation and the related variation of wave intensity using the DAWN code. *Journal of Geophysical Research: Space Physics*, *119*, 3362–3372. https://doi.org/10.1002/2014JA019820

Tsurutani, B. T., Richardson, I. G., Lepping, R. P., Zwickl, R. D., Jones, D. E., & Smith, E. J. (1984). Drift mirror Mode waves in the distant ($X \sim 200$ Re) magnetosheath. *Geophysical Research Letters*, *11*, 1102.

Vedenov, A. A., & Sagdeev, R. Z. (1958). Some properties of a plasma with an anisotropic ion velocity distribution in a magnetic field. In M. A. Leontovich (Ed.), *Plasma physics and the problem of controlled thermonuclear reactions* (Vol. 3, p. 332). Pergamon Press, Hardback.

Wang, Y. L., Elphic, R. C., Lavraud, B., Taylor, M. G. G., Birn, J., Raeder, J., … Friedel, R. H. (2005). Initial results of high-latitude magnetopause and low-latitude flank flux transfer events from 3 years of Cluster observations. *Journal of Geophysical Research*, *110*, A11221. https://doi.org/10.1029/2005JA011150

Wang, Y. L., Elphic, R. C., Lavraud, B., Taylor, M. G. G. T., Birn, J., Russell, C. T., … Zhang, X. X. (2006). Dependence of flux transfer events on solar wind conditions from 3 years of Cluster observations. *Journal of Geophysical Research*, *111*, A04224. https://doi.org/10.1029/2005JA011342

Winterhalter, D., Neugebauer, M., Goldstein, B. E., Smith, E. J., Bame, S. J., & Balogh, A. (1994). Ulysses field and plasma observations of magnetic holes in the solar wind and their relation to mirror-mode structures. *Journal of Geophysical Research*, *99*, 23,371–23,381. https://doi.org/10.1029/94JA01977

Xiao, C. J., Pu, Z. Y., Ma, Z. W., Fu, S. Y., Huang, Z. Y., & Zong, Q.-G. (2004). Inferring of flux rope orientation with the minimum variance analysis technique. *Journal of Geophysical Research*, *109*, A11218. https://doi.org/10.1029/2004JA010594

Xiao, C. J., Pu, Z. Y., Huang, Z. Y., Fu, S.-Y., Xie, L., Zong, Q.-G., … Tao, C. (2004). Multiple flux rope events at the high2latitude magnetopause on January 26, 2001: Current density calculating. *Chinese Journal of Geophysics*, *47*(4), 555–561.

Xiao, T., Shi, Q. Q., Zhang, T. L., Fu, S. Y., Li, L., Zong, Q. G., … Reme, H. (2010). Cluster-C1 observations on the geometrical structure of linear magnetic holes in the solar wind at 1 AU. *Annals of Geophysics*, *28*(9), 1695–1702. https://doi.org/10.5194/angeo-28-1695-2010

Xiao, T., Shi, Q. Q., & Sun, W. J. (2011). Cluster observations of magnetic holes near the interplanetary current sheets at 1 AU, in 2011 30th URSI Gen. Ass. Sci. Symp., pp. 1–3.

Xiao, T., Shi, Q. Q., Tian, A. M., Sun, W. J., Zhang, H., Shen, X. C., & Du, A. M. (2014). Plasma and magnetic-field characteristics of magnetic decreases in the solar wind at 1 AU: Cluster-C1 observations. *Solar Physics*, *289*(8), 3175–3195. https://doi.org/10.1007/s11207-014-0521-y

Yao, S., He, J.-S., Tu, C.-Y., Wang, L.-H., & Marsch, E. (2013). Small-scale pressure-balanced structures driven by mirror-mode waves in the solar wind. *The Astrophysical Journal*, *776*, 94. https://doi.org/10.1088/0004-637X/776/2/94

Yao, S. T., Shi, Q. Q., Li, Z. Y., Wang, X. G., Tian, A. M., Sun, W. J., … Rème, H. (2016). Propagation of small size magnetic holes in the magnetospheric plasma sheet. *Journal of Geophysical Research: Space Physics*, *121*, 5510–5519. https://doi.org/10.1002/2016JA022741

Yao, S. T., Wang, X. G., Shi, Q. Q., Pitkänen, T., Hamrin, M., Yao, Z. H., … Liu, J. (2017). Observations of kinetic-size magnetic holes in the magnetosheath. *Journal of Geophysical Research: Space Physics*, *122*, 1999–2000. https://doi.org/10.1002/2016JA023858

Yao, Z., Rae, I. J., Guo, R. L., Fazakerley, A. N., Owen, C. J., Nakamura, R., … Zhang, X.-J. (2017). A direct examination of the dynamics of dipolarization fronts using MMS. *Journal of Geophysical Research: Space Physics*, *122*, 4335–4347. https://doi.org/10.1002/2016JA023401

Zhang, T. L., Russell, C. T., Baumjohann, W., Jian, L. K., Balikhin, M. A., Cao, J. B., … Vörös, Z. (2008). Characteristic size and shape of the mirror mode structures in the solar wind at 0.72 AU. *Geophysical Research Letters*, *35*, L10106. https://doi.org/10.1029/2008GL033793

Zhang, T. L., Baumjohann, W., Russell, C. T., Jian, L. K., Wang, C., Cao, J. B., … Volwerk, M. (2009). Mirror mode structures in the solar wind at 0.72 AU. *Journal of Geophysical Research*, *114*, A10107. https://doi.org/10.1029/2009JA014103

Zhang, H., Kivelson, M. G., Angelopoulos, V., Khurana, K. K., Pu, Z. Y., Walker, R. J., … Phan, T. (2012). Generation and properties of in vivo flux transfer events. *Journal of Geophysical Research*, *117*, A05224. https://doi.org/10.1029/2011JA017166

Zhang, X.-J., Artemyev, A., Angelopoulos, V., & Horne, R. B. (2017). Kinetics of sub-ion scale magnetic holes in the near-Earth plasma sheet. *Journal of Geophysical Research Space Physics*, *122*, 10,304–10,317. https://doi.org/10.1002/2017JA024197